Energy 308 (2024) 132844

Contents lists available at ScienceDirect

Energy

journal homepage: www.elsevier.com/locate/energy

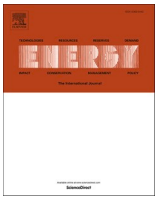

Part-load analysis and preliminary annual simulation of a constant inventory supercritical CO_2 power plant for waste heat recovery in cement industry

Dario Alfani *, Marco Astolfi, Marco Binotti, Paolo Silva, Giacomo Persico

Politecnico di Milano, Energy Department, Milano, Italy

A B S T R A C T

The present work investigates the part-load performance of a MW-scale sCO_2 power plant designed as waste heat recovery unit for an existing cement plant located in Czech Republic, in the framework of the H2020 funded project CO2OLHEAT. The study first presents the selected power plant configuration and then focuses on the evaluation of its part-load operation due to variation of flue gas mass flow rate and temperature. The range of flue gas conditions at the outlet of the upstream process is retrieved from a preliminary statistical analysis of historical trends obtained through the cement plant monitoring. The numerical model developed for this study aims at providing realistic results thanks to the adoption of turbomachinery performance maps provided by the turbomachinery manufacturer of the project. Moreover, heat exchangers have been modelled through a discretized approach which has been validated against manufacturer data, while piping inventory and pressure losses have been assessed through a preliminary sizing that considers the actual distances to be covered in the cement plant. Performance decay is estimated for the whole range of flue gas conditions, reporting the most significant power cycle parameters, and identifying the main causes of efficiency loss. The part-load analysis is carried out considering a constant CO_2 inventory, in order to reduce the system complexity and capital cost and simplify plant operation. Results show that the operation entails minor variation of the compressors operative points in the whole range of operating conditions of the cement plant, avoiding the risk of anti-surge bypass activation. Moreover, the plant is able to work close to the nominal thermodynamic cycle efficiency (20.5 %–23.0 %) for most of the year and benefits from part-load operation in terms of overall performance. In the last part of the work, a preliminary techno-economic analysis of the plant is also presented to highlight the potential advantages of sCO_2 technology for waste heat recovery applications. The results of the part-load performance of the plant are combined with the flue gases data obtained from the preliminary statistical analysis and the cement plant historical monitoring. An annual electricity production equal to 13′909.7 MWh is obtained, corresponding to 6560 equivalent hours and a system capacity factor of 74.9 %. The investment cost of each CO2OLHEAT plant component is estimated by means of cost correlations obtained from literature and the non-discounted payback time is computed as a function of the electricity selling price. The results show that, even considering electricity prices before 2022, the payback time of the CO2OLHEAT plant is estimated to be lower than 8 years, justifying the industrial interest in the proposed technology.

1. Introduction

Waste heat recovery (WHR) systems represent one of the most important technologies to improve the energy efficiency and reduce the carbon footprint of the industrial sector [1,2]. Several studies highlighted the vast WHR potential of the EU industrial sector: for example, Bianchi et al. [3] highlighted how it accounts for 26 % of the total final energy consumption, even if approximately half of this energy (about 1534 TWh_{th}) is dissipated to the environment. In particular, the authors estimated the energy wasted in the form of exhausts and effluents to be 29 % of the total industrial consumption, leading to an available thermal power of 920 TWh_{th}, demonstrating the large potential for waste-heat-to-power applications.

Waste heat conversion technologies have undergone substantial development in the last decades. The Steam Rankine Cycle (SRC) and the Organic Rankine Cycle (ORC) technologies have emerged as the most commonly adopted solutions for converting waste heat into electricity, and the selection between these two options is mostly depending on the heat source temperature and the system size.

SRCs have proven highly effective in larger setups (from tens of MWs) and at higher temperature ranges (above 400 °C), thanks to their efficiency and the utilization of standardized components which leads to a lower investment cost of the WHR system. However, they encounter limitations when dealing with heat sources characterized by smaller available thermal power or lower temperatures, leading to lower conversion efficiencies and the necessity for complex system configurations to compensate for these shortcomings [4].

Conversely, ORCs, utilizing organic compounds as working fluids,

* Corresponding author.
E-mail address: dario.alfani@polimi.it (D. Alfani).

https://doi.org/10.1016/j.energy.2024.132844
Received 4 September 2023; Received in revised form 31 July 2024; Accepted 14 August 2024
Available online 21 August 2024

have seen increased popularity, particularly in the low-to-medium temperature range. Their advantages lie in the reduced number of turbine stages, the possibility to have a dry expansion even starting from saturated vapor conditions, the simpler plant layout, and the opportunity to select the working fluid with the most appropriate pressure levels for each specific application [5]. Yet, organic fluids are generally not suitable to properly harness the potential of heat sources with temperature higher than 400 °C due to their low thermal stability limits [6].

Although the presence of commercial technologies as ORC for small-scale low-temperature applications and SRC for larger and higher temperature systems, a huge market potential is available when waste heat is available at mid-to-high temperature [7,8], as for example in the cement production sector [9]. Supercritical carbon dioxide (sCO_2) power plants are widely recognized as a very promising technology for several applications based on solar energy [10,11], 4th generation nuclear reactors [12,13] and fossil fuels [14,15]. However, this technology has received a wider interest also for waste heat recovery applications [16], thanks to more compact turbomachinery, higher ramp rate, lower minimum load and shorter start-up time than steam power plants [17–19] and better performance with respect to ORCs for heat source temperatures higher than 350–400 °C [7,16].

The practical implementation of sCO_2-based WHR systems has been first proposed by Echogen Power Systems, a US company founded in 2007, and their market sector was mostly focused on medium-to-high temperature (up to 530 °C) applications for several industrial sectors, as petroleum refining, chemical processing and cement, iron, steel, or glass manufacturing. Echogen solution was initially based on a simple recuperated cycle layout, but it then adopted a more complex design, called from the company "Dual Rail configuration", as this configuration allows to obtain a higher power output and a better exploitation of exhaust gases sensible heat [20].

2. Novelty and scope of the work

Numerous publications have then confirmed the viability and the potential of sCO_2 power cycles for WHR applications (for a thorough review it is possible to refer to Refs. [16,21]), yet the literature lacks a complete and detailed analysis of a case-study integrating (i) the nominal design of the plant, (ii) a yearly simulation considering the off-design behavior of the different system components and (iii) an economic analysis highlighting the feasibility of the solution.

This study aims to bridge this gap, and it focuses on the nominal design and the off-design simulation of a sCO_2 power plant conceived as heat recovery unit for an existing cement plant in the framework of the H2020 funded project CO2OLHEAT [22].

The selected cement plant is located in Prachovice, Czech Republic (see Fig. 1), and its operation undergoes variable conditions depending on the load and the activation of raw mills.

This implies a variation in the thermodynamic conditions of the hot flue gas available for the waste heat recovery process, eventually affecting the performance and the operation of the bottoming sCO_2 power unit.

Fig. 1. CEMEX cement manufacturing plant in Prachovice (CZ).

The knowledge of the expected trend for sCO_2 cycle main thermodynamic quantities and operating parameters is of fundamental importance for both finalizing the design of each component and for the definition of the control system ensuring a safe, reliable, and efficient operation of the power plant. Understanding the adaptation of the power plant to the variation of a specific boundary condition requires a properly developed numerical tool and the knowledge of detailed information on the design of the main components, namely the turbomachinery and heat exchangers. This paper aims at providing such information, so as to demonstrate the potential of sCO_2 power units in the cement production sector, supported by components numerical models validated on the data provided by the project consortium industrial partners. Final results also provide useful insights and can guide the design decision of other industrial or residential applications characterized by similar waste heat potential. Moreover, it must be noted that the present work represents only the second analysis available in the literature on off-design performance of sCO_2 cycles considering a constant CO_2 inventory (the other one is [16]), and the first one to consider a practical case-study with heat source data coming from the cement plant monitoring and sCO_2 components modelling validated on manufacturers data. The adoption of a constant CO_2 inventory solution, even if more complex to simulate from a numerical point of view (see Section 4), allows to strongly simplify the day-to-day plant operation, an aspect of crucial importance when dealing with industrial WHR solutions.

The off-design analysis investigates both the effect of flue gas flow rate and temperature variations, which have been retrieved from a preliminary statistical analysis of historical trends obtained from the cement plant monitoring. Mass flow rate of flue gas released from the cement plant is mainly affected by the number of active raw mills, while flue gas temperature varies in a narrow range between 400 °C and 370 °C. The most representative operating conditions of the selected cement plant are reported in Table 1. The nominal flue gas conditions are assumed for the cement plant running with no active raw mills: flue gas flow rate of 230′000 Nm^3/h (occurring approximately 5 % of the year) and flue gas temperature equal to 400 °C.

3. Nominal sCO_2-based power plant design

The nominal design of the power plant is based on the assumptions defined in the framework of the CO2OLHEAT project and agreed with all the consortium partners, including constraints and specifications of component manufacturers as Baker Hughes (BH), Siemens Energy (SIE), Bosal and Heatric. The plant is based on a simple recuperated cycle without neither recompression nor recuperator bypass, as reported in Fig. 1: the choice is motivated by the relatively low maximum temperature of the heat source (i.e., the cement plant flue gas) and the high value of minimum stack temperature to avoid acid condensation (150 °C). First compressor stage inlet conditions (point 1 in Fig. 2) are set to 32 °C and 85 bar to properly exploit the high density of CO_2 in the proximity of the critical point and improve thermodynamic cycle efficiency. Maximum cycle pressure (point 3) is set to 216.9 bar, which

Table 1
Most representative cases of the cement plant operation (in brackets the fraction of time in which each condition occurs in a year).

	T_{FG} = 400 °C	T_{FG} = 370 °C
No raw mills in operation (5 %) 230′000 Nm^3/h of FG available	Case A (nominal)	Case D
One raw mill in operation (85 %) 165′000 Nm^3/h of FG available	Case B	Case E
Two raw mills in operation (10 %) 100′000 Nm^3/h of FG available	Case C	Case F

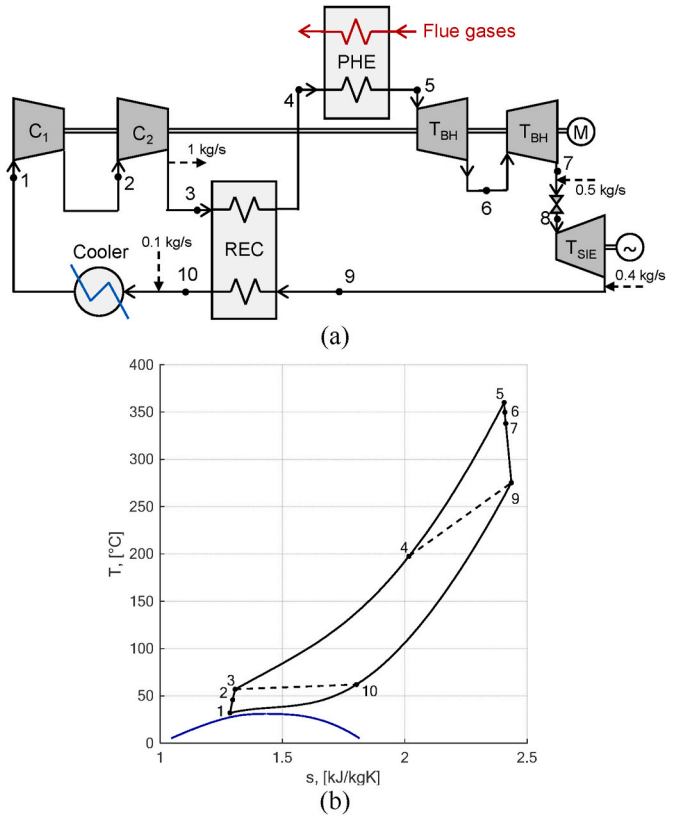

Fig. 2. Layout (a) and T-s (temperature-specific entropy) diagram (b) of the sCO_2 power cycle.

corresponds to a turbine inlet pressure (point 5) of around 210 bar, a value considered a good tradeoff between cycle performance, component manufacturability and techno-economic feasibility. The resulting cycle pressure ratio is equal to 2.55 and it is achieved with two centrifugal compressors in series that have been designed by BH.

3.1. Compressors and turbines design

The compressors are installed on the same shaft and are mechanically driven by two centripetal turbines in series, thus creating a compact turbo-expander unit. A third axial turbine on a separate shaft connected to an alternator is dedicated to the electricity production (power turbine designed by SIE). To ensure a safe start-up of the system and properly balance the power required by the compressors and the power delivered by the centripetal BH turbines in all operating conditions, an electric motor ("helper") is connected to the shaft, absorbing 246 kW of electric power in nominal conditions.

In this study, using a direct flue gas-pressurized CO_2 primary heat exchanger (PHE) has been favored over employing a heat transfer fluid (HTF) loop based on diathermic oil. The goal is to maximize turbine inlet temperature, reduce system complexity and avoid a large inventory of flammable liquid on site, ultimately leading to possible reductions in capital and operating costs related to additional equipment, piping and fire protection. On the other hand, the use of a HTF loop would be preferrable in case of lack of space close to the upstream process or in case of a discontinuous process, where the use of thermal storage would allow to decouple waste heat recovery and power production. According to the choice of direct heat introduction, the maximum temperature (point 5) of the cycle is set at 360 °C, namely 40 °C lower than the flue gas nominal temperature in order to design the primary heat exchanger with a reasonable heat transfer surface.

The CO_2 expansion is then completed in the power turbine (point 8 to 9), which exploits the residual pressure ratio and produces the electrical power output. Power turbine operation can be controlled with an admission valve that involves a pressure drop of 0.3 bar in wide open position.

A CO_2 mass flow rate of 1 kg/s is extracted downstream of the compressors and reintroduced in the power cycle to compensate for Dry Gas Seals (DGS) leakages in turbines (0.5 kg/s for mechanical drive turbine and 0.4 kg/s for power turbine) and injected in minor amount upstream of the cooler (0.1 kg/s). Turbomachinery nominal efficiencies are assumed equal to preliminary values provided by manufacturers: 73 % for the compressors, 84 % for the mechanical-drive turbines, and 82 % for the power turbine.

An additional efficiency loss equal to 5 % is accounted for mechanical and electrical losses for both shafts.

3.2. Heat exchangers and piping

The heat transfer surfaces and internal volumes of the different heat exchangers are calculated by matching the assumed pressure drops by means of numerical routines proprietary of Politecnico di Milano, mostly based on previous experience from the H2020 sCO2-Flex project [23].

For each heat exchanger the numerical code assumes perfect countercurrent flow arrangement and varies the CO_2 velocity to match the specified pressure drop (see Table 2). Each heat exchanger is discretized into 30 sections to properly catch local variations of fluid thermophysical properties and accurately compute the required heat transfer surface. The global heat transfer coefficient (U, related to the internal heat transfer surface) of each HX sub-section is calculated using Equation (1), where the internal (htc_{int}) and external (htc_{ext}) heat transfer coefficients are computed thanks to specific correlations depending on the considered fluid and HX geometry, as reported in Table 3.

Then, using Equation (2) the internal heat transfer area of each section is computed and then summed to obtain the total required heat transfer surface of each heat exchanger.

Finally, by knowing the geometrical features of each component, it is possible to calculate the HX metal masses and internal volumes, as well as the inventory of working fluid contained within each of them, thanks to the knowledge of the CO_2 density in each HX section.

$$U = \left(\frac{1}{htc_{int}} + \frac{d_{int} \cdot \ln\left(\frac{d_{ext}}{d_{int}}\right)}{2k_{metal}} + \frac{1}{\frac{A_{ext,finned}}{A_{ext,plain}} \cdot \frac{A_{ext,plain}}{A_{int}} \cdot htc_{ext}} \right)^{-1} \quad (1)$$

$$A_{HX} = \sum_{i=1}^{30} \frac{\dot{Q}_i}{U_i \Delta T_{lm,i}} \quad (2)$$

The primary heat exchanger consists of a finned tube HX with direct heat transfer between the flue gas, which flows across the finned tubes

Table 2
Main assumption related to the nominal cycle design.

Parameter	Value
Minimum cycle temperature, °C	32
Minimum cycle pressure, bar	85
Maximum cycle pressure, bar	216.9
PHE pinch point temperature difference, °C	40
Cooling water inlet/outlet temperature, °C	20/27
Cooling water Δp, bar	1.5
PHE CO_2 Δp, bar	2
Cooler CO_2 Δp, bar	4
Admission valve nominal Δp, bar	0.3
REC pinch point temperature difference, °C	5
REC hot/cold side Δp, bar	0.75/1.25
BH/SIE turbines isentropic efficiency	84 %/82 %
Compressors isentropic efficiency	73 %
Water pump efficiency	75 %
Mechanical and electrical losses	5 %

Table 3
Main assumption and results related to the nominal heat exchangers design of the CO2OLHEAT plant.

PHE	
HX type	Finned Tube
Tube internal diameter, mm	20
Ratio of tube pitch to external diameter	1.25
Ratio of finned to plain external area	12
Tube material	SS316L
Heat transfer correlation flue gas side	Zukauskas
Heat transfer correlation CO_2 side	Gnielinski
Total internal heat transfer surface, m^2	155.77
Total CO_2 mass in the component, kg	167.91
Recuperator	
HX type	PCHE
Thickness of plate, mm	1.5
Diameter of semi-circular channel, mm	2
Thickness of wall between channels, mm	0.4
Heat exchanger material	SS316L
Heat transfer correlation hot and cold side	Gnielinski
Internal heat transfer surface (one side), m^2	296.50
CO_2 mass in the component (hot/cold), kg	14.47/53.94
Cooler	
HX type	Shell&Tube
Tube internal diameter, mm	20
Tube material	Cu
Heat transfer coefficient water side, W/m^2K	7500
Heat transfer correlation cold side	Gnielinski
Total internal heat transfer surface, m^2	80.48
Total CO_2 mass in the component, kg	181.41

bundles, and the supercritical CO_2 inside the tubes.

Flue gas from cement plants typically contains a high concentration of particulate matter (PM), which can accumulate on heat exchange surfaces, reducing the effectiveness of heat transfer processes. For sake of simplicity and due to the lack of accurate information on the actual amount of PM present in this specific flue gas, this effect has been neglected in the PHE nominal design. However, it has to be noted that, even considering a high fouling resistance equal to 0.881 m^2K/kW (untreated flue gases produced from coal combustion [24]), the global internal heat transfer coefficient would decrease by less than 7.5 %. This implies that the heat transfer surface reported in the work (155.77 m^2) is undersized by the same extent.

The recuperator (REC) is designed as a printed circuit heat exchanger (PCHE) according to the model suggested in Ref. [25], with a pinch point temperature difference of 5 °C and pressure losses on the low pressure (LP) side and high pressure (HP) side of 1.25 bar and 0.75 bar respectively, as suggested by consortium partner Heatric, responsible of the recuperator design.

The cooler is designed as a water-cooled shell-and-tubes heat exchanger assuming the availability of a stream of water or the adoption of a cooling tower water loop, which is often available in large industrial plants. The cooling water inlet temperature is assumed equal to 20 °C with a temperature rise across the heat exchanger of 7 °C in nominal conditions.

The shell-and-tube heat exchanger is designed considering copper as tube material, with the geometrical dimensions reported in Table 3.

The CO_2 and water side pressure drops in the component are estimated at 4 and 1.5 bar, respectively.

Piping length and diameter have been determined by consortium partner Simerom through a preliminary analysis of the distances to be covered in the cement plant. This data is particularly useful for an accurate evaluation of the pressure losses of the sCO_2 power cycle as well as for the estimation of the CO_2 inventory held within the system, equal to 1247.1 kg. More detailed information about the piping length and diameter is reported in Table 4. The resulting net power output is 2.12 MW, with a cycle efficiency of 22.62 % referred to the inlet thermal power and 11 % if referred to the maximum power available from flue gas cooling down to 150 °C, a limit generally imposed to avoid the condensation of acid compounds.

Table 4
Geometrical parameters of the CO2OLHEAT plant piping.

From	To	d_{int} [mm]	L [m]
Cooler	Compressor	241	10
Compressor	Recuperator (cold side)	137	9
Recuperator (cold side)	Primary Heat Exchanger	173	17
Primary Heat Exchanger	1st Turbine (BH)	216	14.5
1st Turbine (BH)	2nd Turbine (Siemens)	216	12
2nd Turbine (Siemens)	Recuperator (hot side)	236	12
Recuperator (hot side)	Cooler	194	8.5

4. Off-design simulation methodology

In this work the use of a CO_2 tank/vessel for active inventory change is not implemented in order to keep the control strategy of the plant as simple as possible and to reduce the system capital cost. From a numerical point of view, the steady-state part-load operating condition is obtained by solving a system of nonlinear equations, each one representing the part-load behavior of a component in the system, namely the turbomachinery and heat exchangers. As the system is totally sealed and thus the total CO_2 mass within it cannot change, an additional system constraint is introduced in the part-load simulation, and it is respected from a numerical point of view by means of the variation of the cycle minimum pressure. Once the off-design problem is solved, the thermodynamic conditions of each sCO_2 stream are estimated and the system power output can be computed. Fig. 3 depicts the simplified flow diagram to compute the constant inventory part-load operation of the plant.

Regarding the cycle components, compressors are operated at fully open (0°) Inlet Guide Vanes (IGV) and their efficiency is calculated based on the operating maps provided in Fig. 4. During off-design operation the first compressor inlet temperature is maintained equal to the nominal value (32 °C) by regulating the cooling water mass flow rate to the cooler, while cycle minimum pressure varies according to the constant inventory operation.

Mechanical drive turbines work in sliding pressure operation: their isentropic efficiency and reduced mass flow rate (see Equation (3)) are characterized with the correlations reported in Fig. 5a as function of the ratio u/c between the peripheral speed u and the spouting velocity c, defined according to Equation (4).

The power turbine operation is computed through the same methodology but using the turbine pressure ratio as the input parameter (see Fig. 5b). The admission valve at power turbine inlet is not employed in

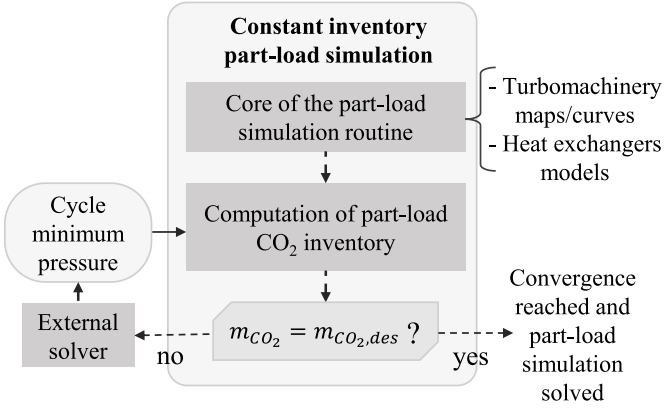

Fig. 3. Simplified flow diagram for the part-load solution of the CO2OLHEAT power cycle under the assumption of constant CO_2 inventory within the system.

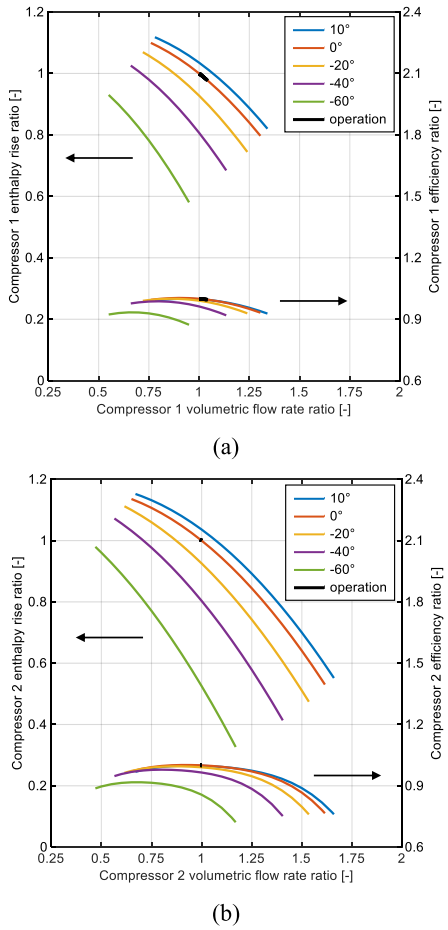

Fig. 4. First (a) and second (b) compressor operating maps (normalized enthalpy rise and efficiency) as function of the normalized volumetric flow rate.

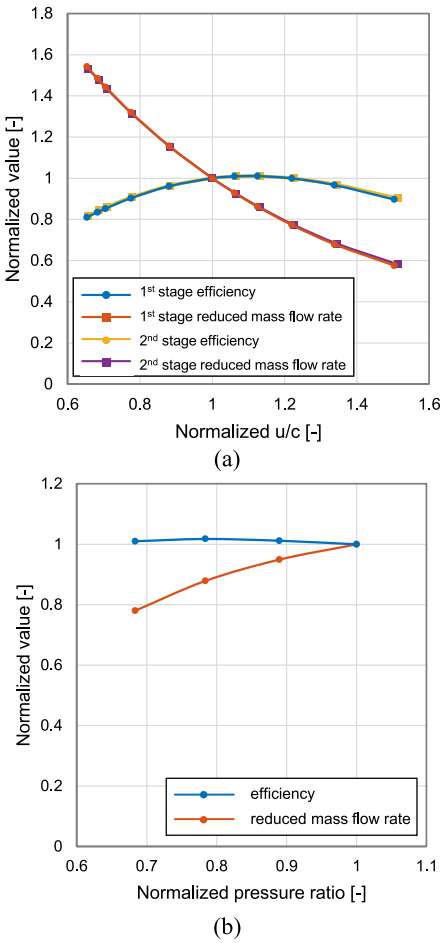

Fig. 5. Baker Hughes (a) and Siemens (b) turbine operating curves (normalized reduced mass flow rate and efficiency) as function of the normalized ratio (u/c) and turbine pressure ratio, respectively.

steady-state operation in order to maximize cycle performance, and CO_2 leakages mass flow rates due to DGS are considered constant and equal to design values for all off-design operation.

Finally, the heat exchangers in off-design conditions are simulated computing the heat transfer coefficients for both the CO_2 and the flue gas using the same correlations proposed for the nominal design (see Table 3), while the pressure drops for each HX side are updated with the simplified correlation reported in Equation (5), where ρ is the local density of the stream.

$$m_{red,turb} = \left.\frac{\dot{m}\sqrt{T}}{p}\right|_{in,turb} \tag{3}$$

$$c = \sqrt{2 \cdot \Delta h_{is,turb}} \tag{4}$$

$$\Delta p = \Delta p_{nom}\left(\frac{\rho_{nom}}{\rho}\right)\left(\frac{\dot{m}}{\dot{m}_{nom}}\right)^2 \tag{5}$$

5. Off-design simulation results

The off-design analysis investigates both the effect of flue gas flow rate and temperature deviation from nominal conditions. In the numerical simulations these two parameters are varied in the following ranges as suggested by the statistical analysis of historical data:

- Flue gas flow rate varies from the nominal value (230′000 Nm^3/h, no raw mills in operation) to 40 % of the nominal value, corresponding to 92′000 Nm^3/h.
- Flue gas temperature varies from the nominal value, equal to 400 °C, to 370 °C.

As the combined effect of the variation of these two flue gas conditions is investigated, the results of the off-design analysis are presented as contour maps displaying how the main parameters and figures of merit of the sCO_2 power cycle vary in off-design operation. Cases A to F (see Table 1) are reported with markers and letters on the displayed maps.

The main figures of merit used to evaluate the system performance are the net cycle thermodynamic efficiency η_{cycle} (including the cooler auxiliaries consumption, namely the cooling water circulation pump, and the electrical helper consumption), the heat recovery factor χ_{rec} and the overall plant efficiency η_{plant}. These parameters are defined in Eq. Eqn 6, Eq. Eqn 8 and Eq. Eqn 9, respectively. It must be noticed that for WHR applications it is not beneficial to maximize the net cycle efficiency but it is important to aim at optimizing the net power output and consequently the overall plant efficiency η_{plant}: this figure of merit not only takes into account the thermodynamic quality of the conversion from heat to electricity (through η_{cycle}), but also the fraction of heat exploited with respect to the total heat available from the heat source (through χ_{rec}). The maximum thermal power made available from the cement plant flues gases has been calculated considering a minimum stack temperature of the exhausts $T_{FG,min}$ equal to 150 °C, a value commonly employed in order to avoid any acid condensation and fouling on heat transfer surfaces [16]. Table 5 reports a summary of the main results for the most representative cases.

Table 5
Summary of the main results for the most representative cases.

	A	B	C	D	E	F
sCO_2 thermodynamic cycle						
CO_2 mass flow rate [kg/s]	45.52	44.31	40.80	44.43	43.06	39.35
Minimum pressure [bar]	85.00	81.78	76.89	82.04	79.36	76.16
Maximum pressure [bar]	216.90	210.26	194.18	210.86	204.05	188.49
CO_2 PHE outlet T [°C]	360.0	334.3	277.8	332.1	308.1	257.4
Heat and power balance						
FG thermal power [MW]	19.76	14.17	8.59	17.39	12.47	7.56
Cycle thermal input [MW]	9.38	9.02	7.81	9.03	8.59	7.25
Compressor 1 power [MW]	0.57	0.56	0.50	0.56	0.54	0.48
Compressor 2 power [MW]	0.55	0.53	0.49	0.53	0.52	0.47
BH turbine power [MW]	0.88	0.83	0.70	0.83	0.78	0.65
Siemens turbine power [MW]	2.42	2.25	1.76	2.24	2.05	1.56
Electric helper power [MW]	0.246	0.261	0.296	0.264	0.279	0.310
Cooling auxiliaries [kW]	52.35	68.32	71.63	66.87	79.61	53.18
Net power output [MW]	2.12	1.92	1.39	1.91	1.69	1.20
Efficiencies						
Cycle efficiency [%]	22.62	21.24	17.83	21.14	19.70	16.53
Heat recovery factor [%]	47.46	63.63	90.87	51.93	68.88	95.91
Overall plant efficiency [%]	10.73	13.52	16.20	10.98	13.57	15.85

$$\eta_{cycle} = \frac{\dot{W}_{net}}{\dot{Q}_{in,cycle}} \tag{6}$$

$$\dot{W}_{net} = \dot{W}_{turb,SIE} - \dot{W}_{helper} - \dot{W}_{cooler,aux} \tag{7}$$

$$\chi_{rec} = \frac{\dot{Q}_{in,cycle}}{\dot{Q}_{FG,max}} = \frac{\dot{m}_{FG} c_{p,FG} \left(T_{FG,max} - T_{stack}\right)}{\dot{m}_{FG} c_{p,FG} \left(T_{FG,max} - T_{FG,min}\right)} \tag{8}$$

$$\eta_{plant} = \frac{\dot{W}_{net}}{\dot{Q}_{FG,max}} = \eta_{cycle} \cdot \chi_{rec} \tag{9}$$

5.1. Heat recovery from the flue gas

The flue gas temperature at PHE outlet is not controlled and tend to decrease during part-load operation (see Fig. 6a) since the PHE heat transfer area is essentially oversized for part-load operating conditions. For this reason, the thermal power input to the cycle decreases less than the flue gas mass flow rate for the same heat source temperature, as reported in Fig. 6b. For example, Case C, characterized by nominal flue gas temperature equal to 400 °C and a reduction of 57 % of the mass flow rate, implies a decrease of heat input to the cycle of only ~17 %. Therefore, during part-load operation the plant tends to exploit a larger fraction of the thermal power available from the exhausts. As a result, reducing the flue gas mass flow rate allows increasing the heat recovery factor χ_{rec} (see Equation Eqn 8 and Fig. 6c) from the nominal value of 47.5 % to a value close to 100 % for case F. This aspect is also clearly visible from the T-Q diagrams (temperature – thermal power) of the PHE which is depicted for case A (nominal), case C (minimum FG flow rate) and F (minimum FG flow rate and minimum temperature) in Fig. 6d. Cases with minimum FG flow rate are characterized by smaller duty but a lower FG minimum temperature and thus a larger heat recovery factor. Moreover, it is also noticeable how the CO_2 temperature at the outlet of PHE (i.e., the maximum cycle temperature) tends to decrease for low flue gas mass flow rates (cases C and F in Fig. 6d).

5.2. Power plant operating conditions

The CO_2 temperature at the outlet of PHE (first turbine inlet temperature) and the CO_2 mass flow rate processed in the power cycle are reported in Fig. 7a and Fig. 7b, respectively. While maximum cycle temperature decreases rapidly when FG mass flow rate reduces, the CO_2 mass flow rate in the power cycle tends to remain fairly constant, as it is proportional to the slope of the CO_2 profile in the T-Q diagram, which remains similar. Its value passes from 45.5 kg/s of the nominal conditions to a value equal to 39.4 kg/s in case F (−11.2 %).

Fig. 7c and Fig. 7d depict the cycle maximum and minimum pressure as function of the flue gas conditions.

It is possible to notice that, as the flue gas mass flow rate and temperature decrease, both pressure levels decrease due to the sliding pressure operation of the turbines and the strong reduction of average CO_2 temperature in the PHE.

The cycle maximum pressure passes from a nominal value of 216.9 bar to a value of 188.5 bar for case F while, for the same case, the minimum pressure decreases from 85 bar to 76.2 bar.

On the other hand, the cycle pressure ratio variation in the whole off-design operation is limited, with a variation range restricted between 2.48 and 2.57 (−3.0 % and +0.8 % with respect to nominal conditions, respectively).

5.3. Turbines, generator and electrical helper operation

Fig. 8a depicts the power required by the electric helper balancing the turbo-expander shaft. The electric consumption increases from 246 kW (Case A, nominal condition) to 310 kW (Case F), mainly due to the decrease of the maximum cycle temperature (i.e., the first turbine inlet temperature) at nearly constant cycle pressure ratio. Maximum cycle temperature reduction leads to a consequent decrease of CO_2 temperature at power turbine inlet (Fig. 8c) and a reduction of its specific work as it can be seen from Fig. 8d, where power turbine isentropic enthalpy drop varies from a design point condition of 69.0 kJ/kg to a value of 50.8 kJ/kg (−26.4 %) in case F. As a consequence, although the CO_2 mass flow rate is little affected, the SIE turbine power output appreciably decreases from more than 2.4 MW in the design condition down to slightly less than 1.6 MW in condition F (see Fig. 8b).

5.4. Compressors operation

Considering the whole range of off-design operation of the plant, while the first compressor operating point deviates slightly from the nominal conditions, for the second compressor the variation is almost negligible, as noticeable from Fig. 4a and Fig. 4b, respectively. This aspect is due to the almost constant volumetric flow rate at both compressors inlet, due to the combined effect of the slight decrease of both the CO_2 mass flow rate and the cycle minimum pressure, which cause a consequent reduction of the inlet density to the compressors (Fig. 9a and Fig. 9b).

Therefore, the efficiency variation during off-design operation of the compressors is very limited, leaving the specific consumption of these components practically unaffected by the variation of the cement plant flue gas conditions. Furthermore, this aspect leads to a significantly easier operation of such components and allows to use the installed IGVs only to manage the startup of the power plant.

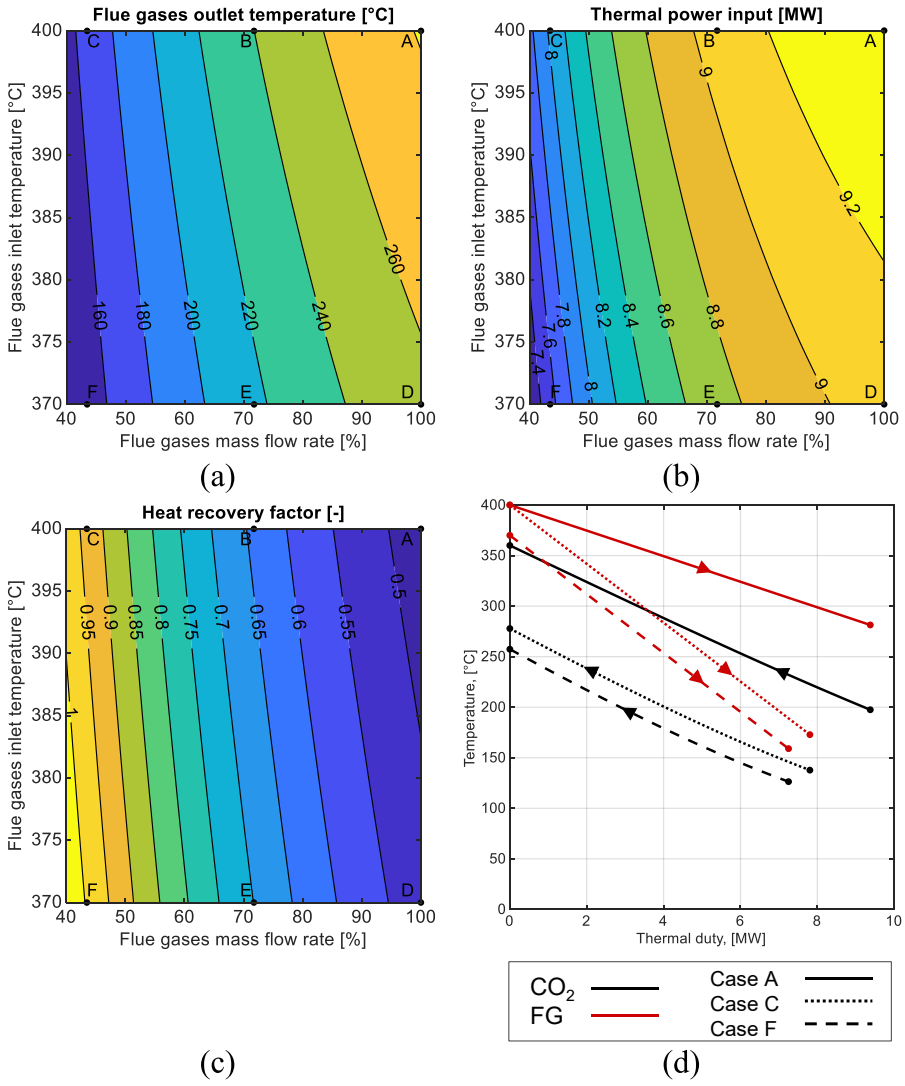

Fig. 6. Flue gas temperature at PHE outlet (a), thermal power transferred in the PHE (b) and heat recovery factor as function of the off-design flue gas conditions. PHE T-Q (temperature - thermal power) diagram for cases A, C, F (d).

5.5. Net power output and cycle performance

In part-load operation cycle efficiency (Fig. 10b) decreases from a nominal value of 22.6 % (case A) to a minimum value of 16.5 % (case F), corresponding to −27 % in relative terms. However, the performance decay is not constant across the whole range of operation and there is a wide span of conditions where the performance remains close to the nominal one. In particular, considering the actual cement plant operation, the sCO_2 power system can be operated with a conversion efficiency around 20 % for most of the year, as the cases B and E, which represent 85 % of the yearly operation, feature a cycle efficiency of 21.2 % and 19.7 %, respectively. On the other hand, in these two conditions the waste heat recovery plant can achieve a lower net power output, ranging from 1.69 MW to 1.92 MW. Considering the whole range of the cement plant operation, the net power output (Fig. 10a) decreases from a nominal value of 2.12 MW down to 1.20 MW (−43.4 %) of electricity generated in the most penalizing condition (case F), as a consequence of the consumption increase of the electric helper installed on the turbo-expander shaft, as well as of the decrease of SIE power turbine electric output.

Nevertheless, this result can be considered encouraging as it is obtained with both a reduction of the available flue gas mass flow rate, equal to −56.5 %, and a decrease of 30 °C of their maximum temperature, leading to an overall decrease of the available thermal power of −61.7 %. Eventually, it is possible to notice that the overall plant efficiency (Fig. 10c), defined as the product of the cycle efficiency and the heat recovery factor, increases in part-load operation, and presents a maximum close to case C (around 16.2 % vs. 10.7 % in nominal conditions, equal to +51.0 % in relative terms), thanks to the improvement in the heat source exploitation. In this condition, the flue gases have a stack temperature close to the temperature limit to avoid the formation of acid condenses (150 °C, as noticeable from Fig. 6a).

6. Economic analysis and preliminary annual simulation

In this section a preliminary evaluation of the capital cost for the CO2OLHEAT sCO_2 power plant is carried out. The investment cost of each plant component is estimated by means of a specific cost correlation obtained from literature: the main set of adopted cost correlations is retrieved from Weiland et al. [26], which is then integrated with cost correlations for the sCO_2/exhaust heat exchanger (PHE) and for the water-cooler from Wright et al. [27] and from Astolfi [28], respectively. Finned tube heat exchanger cost depends only on the overall UA value of the component while, on the contrary, shell-and-tube HXs cost correlation depends on both heat transfer area and pressure. For each component an installation factor ranging from 5 % to 20 % has been then

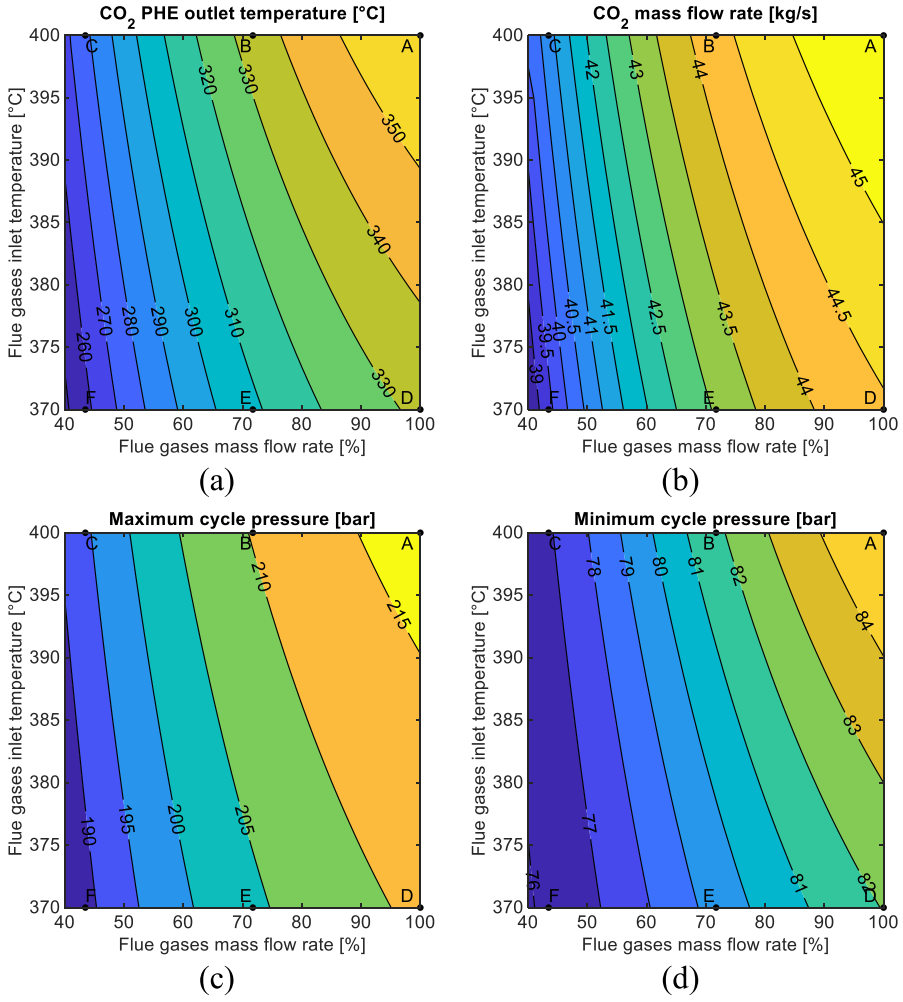

Fig. 7. CO_2 temperature at PHE outlet (a), CO_2 mass flow rate processed by the cycle (b), cycle maximum (c) and minimum pressure (d) as function of the off-design flue gas conditions.

applied to account for the labor and material costs [26]. All the employed cost correlations adopt dollar [$] as currency and their estimates have then been converted into euro [€] currency with an exchange rate equal to 0.93 €/$. A contribution equal to 20 % of the equipment-only cost is accounted for the balance of plant (BOP), mainly including piping, instrumentation, and control costs. Contingencies and engineering, procurement, and construction (EPC) costs are assumed equal to 7 % and 13 % of the bare erected costs [29]. Table 6 reports the cost breakdown for each component of the CO2OLHEAT system investment cost. As cost correlations related to sCO_2 power cycle components are characterized by significant uncertainties, the uncertainty range (UR) for each component has been added to Table 6. Their value has been retrieved from the respective references. Their impact has then been computed considering the minimum and maximum value of the uncertainty associated with each of the components and summing their contributions to obtain the uncertainty related to the total investment cost estimate. It is important to highlight that the turbomachinery size investigated in this work is below the minimum size of cost correlations obtained from literature: 10 MW for axial turbines, as the Siemens power turbine; 8 MW for radial turbines, as the Baker Hughes mechanical drive turbines and 1.5 MW for the compressors. Consequently, the costs of these pieces of equipment are extrapolated with possible inaccuracies in the economic evaluation, probably leading to higher specific costs and therefore to conservative estimates for the CO2OLHEAT plant overall investment cost.

Nevertheless, the system specific cost is estimated at around 2544 €/kW_{el} (with an uncertainty range between 1622.23 €/kW_{el} and 3527.6 €/kW_{el}), a value in the same range of waste heat recovery ORC for the considered power output, which is estimated at around 2000–4000 €/kW_{el} [30].

6.1. Anual electricity generation assessment

Finally, the results of the part-load performance of the plant have been combined with the flue gases data obtained from the preliminary statistical analysis and the cement plant historical monitoring. The results of this analysis are reported in the two histograms of Fig. 11, where the frequency distribution of the flue gases flow rate and temperature are represented considering a discretization of 1 min. The 1-min timestep trends of these two variables have then been coupled with the information obtained through the performance map reported in Fig. 10a, where the net power output of the plant is depicted in a contour plot as function of the flue gases conditions. In such a way it has been possible to preliminary estimate the electricity yield of the plant and its equivalent hours, as well as first indications about the techno-economic performance of the system and its feasibility and financial convenience. Eventually, by summing up the electricity production of each timestep an annual electricity yield of 13′909.7 MWh has been obtained, equivalent to 6560 equivalent hours and a capacity factor of 74.9 %.

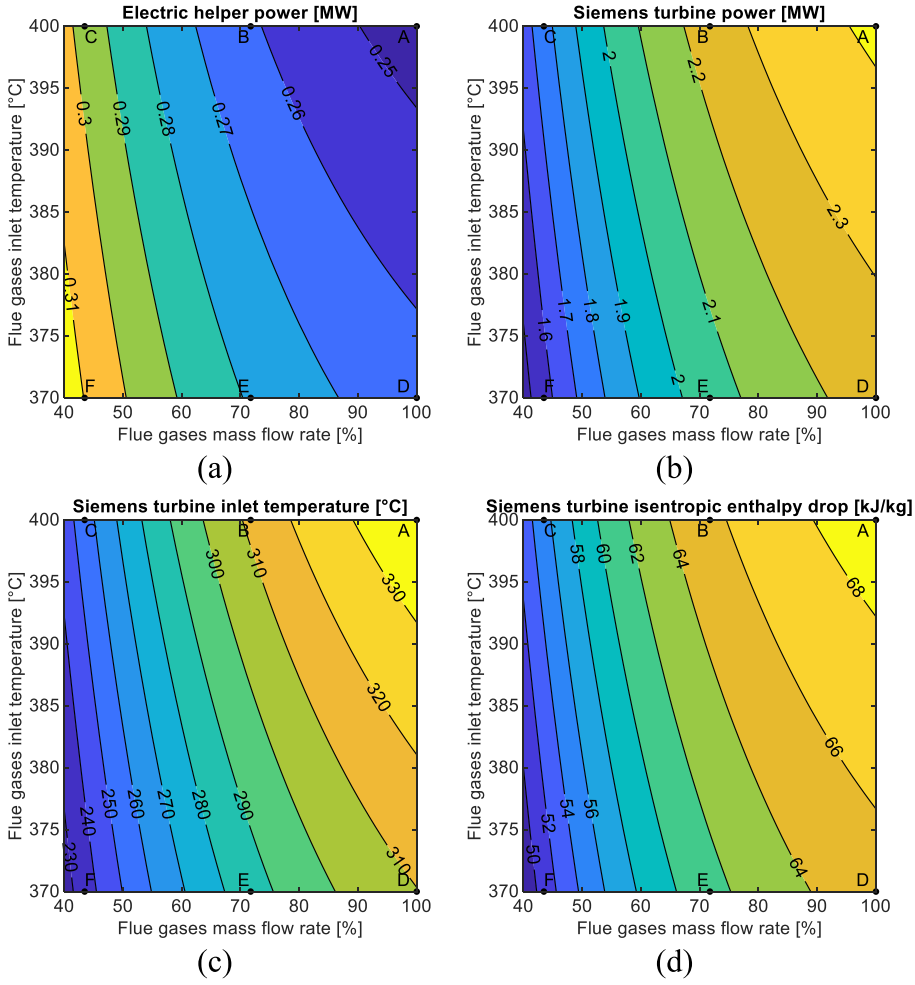

Fig. 8. Electric helper power consumption (a), Siemens turbine power (b), Siemens turbine inlet temperature (c) and isentropic enthalpy drop (d) as function of the off-design flue gas conditions.

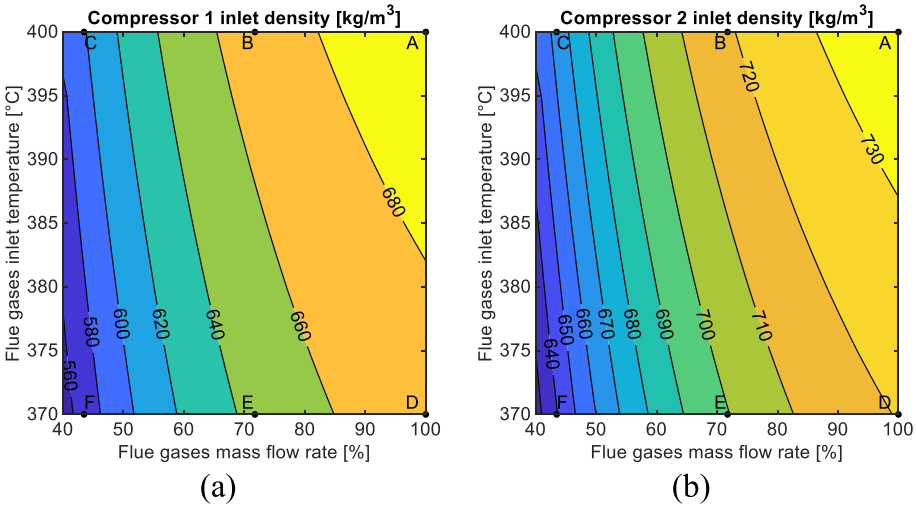

Fig. 9. First (a) and second (b) compressor CO_2 inlet density as function of the off-design flue gas conditions.

6.2. *Preliminary economic analysis*

Finally, a preliminary economic analysis of the profitability of the proposed technology is presented in order to highlight the effects on the non-discounted payback time (PBT) of different assumptions related to the electricity selling price. An annual overall operation and maintenance (O&M) cost equal to 3 % of the total investment cost has been assumed for the turbomachinery and heat exchangers maintenance as well as for CO_2 renewal.

According to the large electricity needs of a cement manufacturing

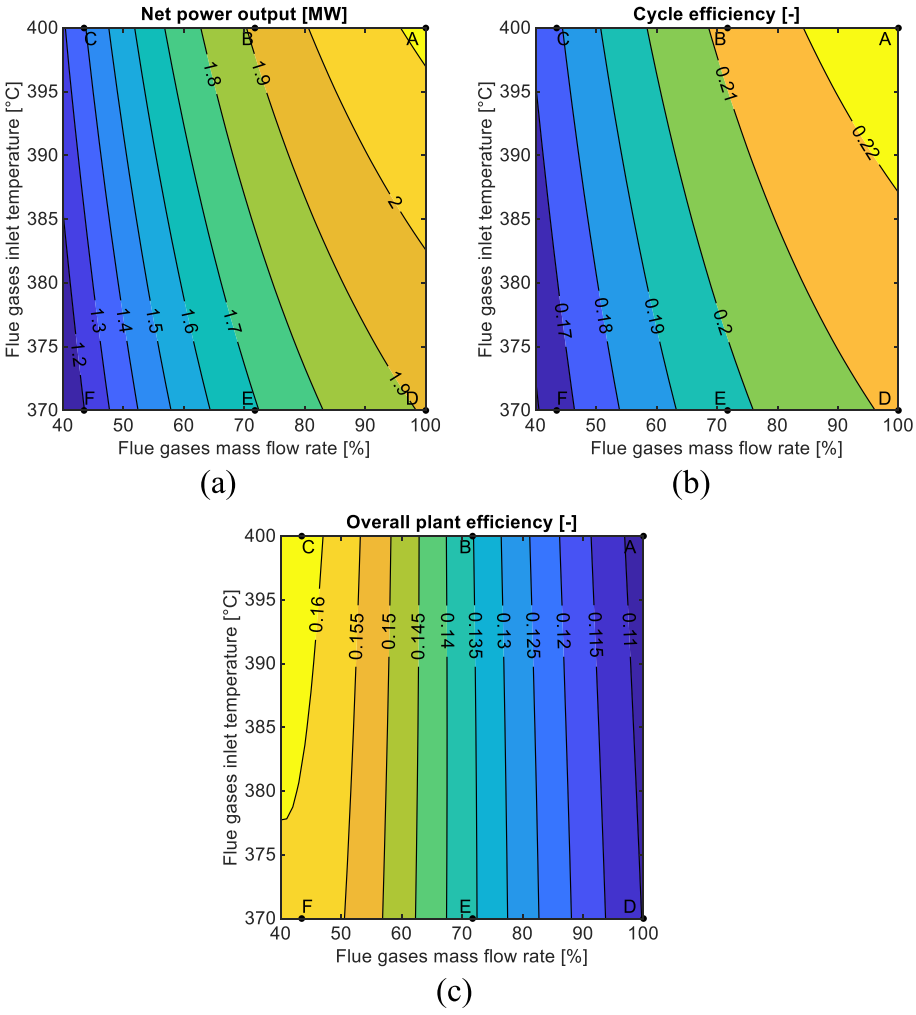

Fig. 10. Net power output of the plant (a), cycle efficiency (b) and overall conversion efficiency (c) as function of the off-design flue gas conditions.

Table 6
Cost breakdown of the different components of the cycle with the uncertainty range (UR) related to their cost and their effect on the economic results (uncertainty ranges are reported in *italic* inside square brackets).

Component	Cost [M€]	Share	UR
PHE	0.86	13.2 %	*−50/+30 %*
BH turbine	0.42	6.6 %	*−32/+51 %*
SIE turbine	0.34	5.3 %	*−25/+28 %*
Generator	0.19	2.9 %	*−19/+23 %*
Compressors	1.44	22.2 %	*−40/+48 %*
Electrical helper	0.06	0.9 %	*−15/+20 %*
Recuperator	1.05	16.2 %	*−31/+38 %*
Cooler	0.14	2.2 %	*−30/+30 %*
Piping and BOP	0.90	13.9 %	
Contingency	0.38	5.8 %	
EPC	0.70	10.8 %	
Total IC [M€]		**6.48** [*4.12/9.01*]	
Specific cost [€/kW$_{el}$]		**2544.4** [*1618.0/3537.6*]	

plant, it has been assumed that all the electricity generated by the CO2OLHEAT system is used for self-consumption. Fig. 12 reports the results of this analysis together with their uncertainty range related to the uncertainty on the overall investment cost estimate: the non-discounted PBT varies from approximately 13 years for a non-household electricity price of 50 €/MWh to less than 2 years for 250 €/MWh. The figure also reports the six-month average electricity prices paid by industrial users in Czech Republic starting from 2021 (data for the second semester of 2023 is still not available). Even considering electricity prices before 2022, which has been characterized by a sudden increase of fossil fuels price due to the Russian invasion of Ukraine, it is possible to notice that the PBT of the CO2OLHEAT plant results to be lower than 8 years. These results indicate that, based on current energy prices and economic conditions, the interest in the CO2OLHEAT technology is more than justifiable from an economical point of view, especially considering that these estimates are for a first-of-a-kind plant, and that the investment cost of the different sCO$_2$ power cycles components is expected to drop as the technology becomes more mature.

7. Conclusions

This paper presents the numerical assessment of the part-load performance of a sCO$_2$ power plant for a waste heat recovery application in a cement plant, in the frame of the H2020 funded project CO2OLHEAT. This study demonstrates the possibility to operate waste heat recovery unit based on sCO$_2$ power cycles at constant CO$_2$ inventory. This solution not only allows to decrease the installation cost, but also largely simplifies the system operation at part-load and the power plant control system. Numerical results show how the pressure ratio and CO$_2$ mass flow rate remain relatively constant in the whole range of the cement plant operation, allowing to limit turbomachinery off-design performance decay. As a result, even operating the compressors with fixed IGV aperture, their operative points remain very close to nominal conditions, limiting the issues related to loss of performance and anti-surge bypass

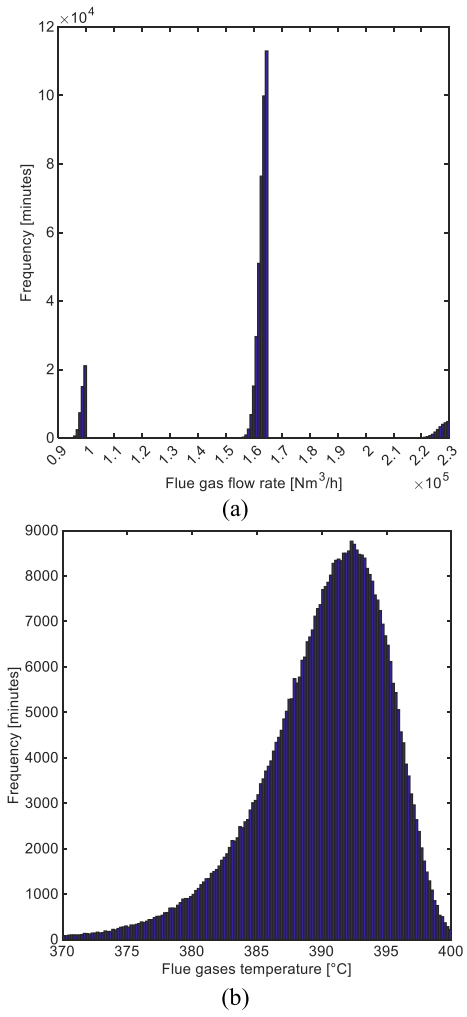

Fig. 11. Flue gases flow rate (a) and temperature (b) frequency distribution for the analyzed operating year of the CEMEX cement manufacturing plant in Prachovice (CZ).

activation. This leads to the possibility of operating the plant for most of the year (90 %) with an efficiency close to the nominal one.

Furthermore, despite a reduction of the cycle conversion efficiency at part-load operation, the overall plant efficiency increases as the sCO_2 power cycle tends to exploit a larger fraction of the thermal power available from the exhausts.

For example, by reducing the flue gas mass flow rate by more than 50 % at the nominal temperature, even if the cycle efficiency decreases by approximately 5 points (from the nominal value of 22.6 % to17.8 %), the heat recovery factor almost doubles (from 47.5 % to 90.9 %), thus resulting in an overall plant efficiency increase of more than 50 % in relative terms (from 10.7 % to 16.2 %). These results will provide useful insights in the next steps of the CO2OLHEAT project, in particular to guide the definition of power plant control system.

The results of the part-load performance of the plant have then been combined with the flue gases data obtained from the preliminary statistical analysis and the cement plant historical monitoring. An annual electricity production equal to 13′909.7 MWh has been obtained, corresponding to 6560 equivalent hours and a system capacity factor of 74.9 %.

Finally, a preliminary techno-economic analysis of the plant is also presented to highlight the potential advantages of sCO_2 technology for waste heat recovery applications. The investment cost of each CO2OLHEAT plant component is estimated by means of cost correlations obtained from literature and the non-discounted payback time is computed

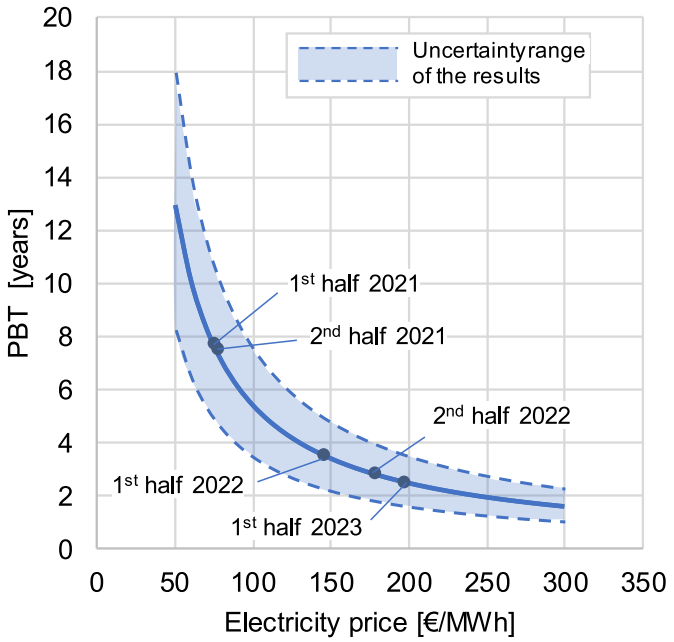

Fig. 12. Non-discounted PBT for the CO2OLHEAT power plant as function of the non-household electricity price. The dark blue dots represent the actual average non-household electricity price in Czech Republic for the considered time interval (*Eurostat data*). The light blue area represents the uncertainty on the PBT obtained using the components costs uncertainty ranges reported in Table 6. (For interpretation of the references to colour in this figure legend, the reader is referred to the Web version of this article.)

as a function of the electricity price. The results show that, even considering electricity prices before 2022, the calculated PBT of the CO2OLHEAT plant is lower than 8 years. Therefore, it can be stated that the industrial interest in CO2OLHEAT technology is more than justifiable even from a techno-economical perspective.

CRediT authorship contribution statement

Dario Alfani: Writing – review & editing, Writing – original draft, Software, Methodology, Formal analysis, Conceptualization. **Marco Astolfi:** Writing – review & editing, Writing – original draft, Supervision, Methodology, Conceptualization. **Marco Binotti:** Writing – review & editing, Supervision. **Paolo Silva:** Writing – review & editing, Supervision, Project administration, Funding acquisition. **Giacomo Persico:** Writing – review & editing, Supervision, Project administration, Funding acquisition.

Declaration of competing interest

The authors declare the following financial interests/personal relationships which may be considered as potential competing interests: Dario Alfani reports financial support was provided by European Union.

Data availability

Data will be made available on request.

Acknowledgements

The CO2OLHEAT project has received funding from the European Union's Horizon 2020 research and innovation programme under grant agreement N° 101022831.

This study was carried out within the NEST - Network 4 Energy Sustainable Transition (D.D. 1243 August 02, 2022, PE00000021) and

received funding under the National Recovery and Resilience Plan (NRRP), Mission 4 Component 2 Investment 1.3, funded from the European Union - NextGenerationEU. This manuscript reflects only the authors' views and opinions, neither the European Union nor the European Commission can be considered responsible for them.

Nomenclature

List of abbreviations

BH – Baker Hughes
DGS – Dry Gas Seals
EU – European Union
FG – Flue gas
HP – High Pressure
HTF – Heat Transfer Fluid
HX or HE – Heat Exchanger
IGV – Inlet Guide Vanes
O&M – Operation and Maintenance
ORC – Organic Rankine Cycle
LP – Low Pressure
PBT – Pay Back Time
PCHE – Printed Circuit Heat Exchanger
PHE – Primary Heat Exchanger
PM – Particulate Matter
sCO2 – supercritical CO_2
S&T – Shell and Tube
SIE – Siemens
UR – Uncertainty Range
WHR – Waste Heat Recovery

List of symbols

c – Spouting velocity [m/s]
c_p – Specific heat capacity [kJ/kgK]
d – diameter [mm]
h – Specific enthalpy [kJ/kg]
m – Mass [kg]
$\dot{m}$ – Mass flow rate [kg/s]
$m_{red,turb}$ – Turbine reduced mass flow rate
L – Length [m]
p – Pressure [bar]
Q or $\dot{Q}$ – Thermal Power [MW]
s – Entropy [kJ/kgK]
T – Temperature [°C]
u – Peripheral speed [m/s]
$\dot{V}$ - Volumetric flow rate [m^3/h]
ρ – Density [kg/m^3]
χ_{rec} – Heat recovery factor [−]
η_{cycle} – Net cycle thermodynamic efficiency [−]
η_{plant} – Overall plant efficiency [−]

References

[1] U.S. Department of Energy. Waste heat recovery: technology opportunities in the US industry. 2008.
[2] Papapetrou M, Kosmadakis G, Cipollina A, La Commare U, Micale G. Industrial waste heat: estimation of the technically available resource in the EU per industrial sector, temperature level and country. Appl Therm Eng July 2017;138:207–16. https://doi.org/10.1016/j.applthermaleng.2018.04.043.
[3] Bianchi G, et al. Estimating the waste heat recovery in the European Union Industry. Energy Ecol. Environ. 2019;4(5):211–21. https://doi.org/10.1007/s40974-019-00132-7.
[4] Raab F, Klein H, Opferkuch F. Steam Rankine cycle instead of organic Rankine cycle for distributed high temperature waste heat recovery – pros and cons. In: 6th International Seminar on ORC power systems; 2021. p. 1–10. https://doi.org/10.14459/2021mp1633019.
[5] Macchi E, Astolfi M. Organic rankine cycle (ORC) power systems. Elsevier Science; 2016.
[6] Invernizzi CM, Bonalumi D. Thermal stability of organic fluids for Organic Rankine Cycle systems. In: Organic rankine cycle (ORC) power systems: technologies and applications; 2017. https://doi.org/10.1016/B978-0-08-100510-1.00005-3.
[7] Astolfi M, Alfani D, Lasala S, Macchi E. Comparison between ORC and CO2 power systems for the exploitation of low-medium temperature heat sources. Energy Oct. 2018;161:1250–61. https://doi.org/10.1016/j.energy.2018.07.099.
[8] White MT, Bianchi G, Chai L, Tassou SA, Sayma AI. Review of supercritical CO2 technologies and systems for power generation. Appl Therm Eng Feb. 2021;185:116447. https://doi.org/10.1016/j.applthermaleng.2020.116447. July 2020.
[9] International Finance Corporation and Institute for Industrial Productivity, "Waste heat recovery for the cement sector: market and supplier analysis." doi: 10.4067/s0718-40262009000600007.
[10] Alfani D, Neises T, Astolfi M, Binotti M, Silva P. Techno-economic analysis of CSP incorporating sCO2 Brayton power cycles: trade-off between cost and performance. AIP Conf Proc 2022. https://doi.org/10.1063/5.0086353.
[11] Neises T, Turchi C. Supercritical carbon dioxide power cycle design and configuration optimization to minimize levelized cost of energy of molten salt power towers operating at 650 °C. Sol Energy 2019;181:27–36. https://doi.org/10.1016/j.solener.2019.01.078. November 2018.

[12] Sienicki JJ, Moisseytsev A, Krajtl L. A supercritical CO2 brayton cycle power converter for a sodium-cooled fast reactor small modular reactor. In: ASME 2015 nuclear forum. American Society of Mechanical Engineers; Jun. 2015. p. 1–10. https://doi.org/10.1115/NUCLRF2015-49185.
[13] Dostal V. A supercritical carbon dioxide cycle for next generation nuclear reactors. Massachusetts Institute of Technology; 2004.
[14] Alfani D, Astolfi M, Binotti M, Silva P. Part-load strategy definition and preliminary annual simulation for small size sCO2-based pulverized coal power plant. J Eng Gas Turbines Power 2021;143(9). https://doi.org/10.1115/1.4051003.
[15] Allam RJ, et al. High efficiency and low cost of electricity generation from fossil fuels while eliminating atmospheric emissions, including carbon dioxide. Energy Proc 2013;37:1135–49. https://doi.org/10.1016/j.egypro.2013.05.211.
[16] Alfani D, Binotti M, Macchi E, Silva P, Astolfi M. sCO2 power plants for waste heat recovery: design optimization and part-load operation strategies. Appl Therm Eng Aug. 2021;195(April 2021):117013. https://doi.org/10.1016/j.applthermaleng.2021.117013.
[17] Persichilli M, Kacludis A, Zdankiewicz E, Held T. Supercritical CO2 power cycle developments and commercialization: why sCO2 can displace steam ste am. Power-Gen India Cent. Asia 2012:1–15.
[18] Alfani D, Astolfi M, Binotti M, Campanari S, Casella F, Silva P. Multi objective optimization of flexible supercritical CO2 coal-fired power plants. Presented at the ASME turbo expo 2019: turbomachinery technical conference and exposition. American Society of Mechanical Engineers Digital Collection; Nov. 2019. https://doi.org/10.1115/GT2019-91789.
[19] Casella F, Mangola G, Alfani D. sCO2-Flex deliverable D5.6 – final report on open-loop plant dynamics. Deliverable; 2021.
[20] Held TJ. Supercritical CO2 cycles for gas turbine combined cycle power plants. In: Power gen international december 8-10, las vegas. Nevada; Dec. 2015. echogen.com/_CE/pagecontent/Documents/Papers/Supercritical%20CO2%20Cycles%20for%20Gas%20Turbine%20Combined%20Cycle%20Power%20Plants.pdf.
[21] Marchionni M, Bianchi G, Tassou SA. Review of supercritical carbon dioxide (sCO2) technologies for high-grade waste heat to power conversion. SN Appl Sci Mar. 2020;2(4):611. https://doi.org/10.1007/s42452-020-2116-6.
[22] "CO2OLHEAT: Supercritical CO2 power cycles demonstration in Operational environment Locally valorising industrial Waste Heat. Available online at: https://co2olheat-h2020.eu/".
[23] "sCO2-Flex: Supporting the electricity system by making fossil fuel based electricity production more flexible. Available online at:https://sco2-flex.eu.".
[24] Shah RK, Sekulić DP. Fundamentals of heat exchanger design. first ed. Wiley; 2003. https://doi.org/10.1002/9780470172605.
[25] Dostal V, Hejzlar P, Driscoll MJ. The supercritical carbon dioxide power cycle: comparison to other advanced power cycles. Nucl Technol 2006;154(3):283–301. https://doi.org/10.13182/NT06-A3734.
[26] Weiland NT, Lance BW, Pidaparti SR. SCO2 power cycle component cost correlations from DOE data spanning multiple scales and applications. Proc. ASME Turbo Expo 2019;9:1–17. https://doi.org/10.1115/GT2019-90493.
[27] Wright SA, Davidson CS, Scammell WO. Thermo-economic analysis of four sCO2 waste heat recovery power systems. 5th int. Symp. - supercrit. CO2 power cycles. 2016. p. 1–16.
[28] Astolfi M. "An innovative approach for the techno-economic optimization of Organic Rankine Cycles. Ph.D. Dissertation.," Italy; 2014.
[29] Blair, N.; Dobos, A.; Freeman, J.; Neises, T.; Wagner, M.; Ferguson, T.; Gilman, P.; Janzou, S. (2014). System Advisor Model™, SAM™ 2014.1.14: General Description. NREL/TP-6A20-61019. National Renewable Energy Laboratory. Golden, CO. Accessed August 28, 2024. https://www.nrel.gov/docs/fy14osti/61019.pdf.
[30] Lemmens S. A perspective on costs and cost estimation techniques for organic Rankine cycle systems. Proc. 3rd int. Semin. ORC power syst.. 2010. p. 1–10. 2015.